

# Two–Loop Neutrino Mass Generation through Leptoquarks

K.S. Babu<sup>\*</sup> and J. Julio<sup>†</sup>

*<sup>a</sup>Department of Physics  
Oklahoma State University  
Stillwater, OK 74078, USA*

## Abstract

We present a new model of radiative neutrino mass generation wherein TeV scale leptoquark scalars induce tiny neutrino masses as two–loop radiative corrections. The neutrino oscillation parameter  $\sin^2 \theta_{13}$  is predicted to be close to the experimental limit within the model. Rare lepton flavor violating processes mediated by leptoquarks have an interesting pattern:  $\mu \rightarrow e\gamma$  may be suppressed, while  $\mu \rightarrow 3e$  and  $\mu - e$  conversion in nuclei are within reach of the next generation experiments. New CP violating contributions to  $B_s - \bar{B}_s$  mixing via leptoquark box diagrams are in a range that can explain the recently reported discrepancy with the standard model.  $D_s^- \rightarrow \ell^- \nu$  decays mediated by leptoquarks brings theory and experiment closer, removing an observed  $2.5 \sigma$  anomaly. Muon  $g-2$  receives new positive contributions, which can resolve the discrepancy between theory and experiment. The leptoquarks of the model are accessible to the LHC, and their decay branching ratios probe neutrino oscillation parameters.

---

<sup>\*</sup>Email: babu@okstate.edu

<sup>†</sup>julio.julio@okstate.edu

# 1 Introduction

It has now been firmly established that neutrinos have tiny masses and that oscillation occurs between different flavors. The standard paradigm that explains the small masses is the seesaw mechanism [1], which generates the effective dimension-5 operator  $\mathcal{O}_1 = (LLHH)/M$ , suppressed by the mass scale  $M$  of the heavy right-handed neutrino. Oscillation data suggests that in this scenario  $M \sim 10^{14}$ , which is well beyond the reach of foreseeable experiments for direct scrutiny. One has to rely on other indirect hints, such as charged lepton flavor violation in a supersymmetric context, in order to falsify this theory.

An interesting alternative to the high scale seesaw mechanism is to induce small neutrino masses at the loop level. The smallness of neutrino masses can be understood as originating from loop and chirality suppression factors. The simplest among this class of models is the Zee model [3] where neutrino masses are induced as one-loop radiative corrections arising from the exchange of charged scalar bosons. The effective operator in this model is  $LLLe^cH/M$ . To convert this to neutrino mass, a loop diagram is necessary.<sup>1</sup> In a second class of models, neutrino masses arise as two-loop radiative corrections via the exchange of singly and doubly charged scalars [5, 6]. The effective operator of these models is  $LLLe^cLe^c/M^2$ . Phenomenology of these models have been studied in Ref. [7].

A classification of low dimensional effective  $\Delta L = 2$  lepton number violating operators that can lead to neutrino masses has been given in Ref. [8]. Among these is an operator labeled  $\mathcal{O}_8$ :

$$\mathcal{O}_8 = L_\alpha \bar{e}^c \bar{u}^c d^c H_\beta \epsilon^{\alpha\beta} \quad (1)$$

where  $\alpha, \beta$  are  $SU(2)_L$  indices. It is the purpose of this paper to develop a renormalizable model that generates  $\mathcal{O}_8$ . We will show that such a model can be consistently constructed, with a variety of testable predictions.

Operator  $\mathcal{O}_8$  is most directly induced by the exchange of scalar leptoquarks.<sup>2</sup> For neutrino mass generation the two quark fields and the charged lepton field in  $\mathcal{O}_8$  will have to be removed, which implies that the masses arise at the two-loop level. The order of magnitude of the induced neutrino masses is

$$m_\nu \sim \frac{m_t m_b m_\tau \mu v}{(16\pi^2)^2 M_{LQ}^4}, \quad (2)$$

where  $\mu$  is a dimensionful coefficient of a cubic scalar coupling, and  $v = 174$  GeV is the electroweak vacuum expectation value (VEV). In order to generate  $m_\nu \sim 0.05$  eV, it is clear that  $M_{LQ}$  must be of order TeV, which would be within reach of the LHC.

TeV scale leptoquarks can mediate a variety of flavor changing processes. We have examined these constraints and found the neutrino mass generation to be self-consistent. Our findings

---

<sup>1</sup>This model is now excluded by neutrino oscillation data (see Ref. [4]).

<sup>2</sup>Neutrino mass generation at the one-loop level by leptoquark exchange has been studied in Ref. [9].

include several interesting features: (i)  $\mu \rightarrow e\gamma$  may be suppressed, because of a GIM-like cancelation, but  $\mu \rightarrow 3e$  and  $\mu - e$  conversion nuclei are within reach of the next generation of experiments. (ii) There is a new CP violating contribution mediated by leptoquark box diagrams in  $B_s - \bar{B}_s$  mixing, which can nicely fit the recently reported anomaly. (iii) The  $2.5\sigma$  discrepancy between theory and experiment in the leptonic decay of  $D_s^\pm$  mesons can be explained in the model, owing to new contributions from the leptoquarks. (iv) Muon  $g - 2$  receives new positive contributions which can resolve the theoretical anomaly there. (v) Neutrino oscillation parameters can be probed in the branching ratios the the leptoquarks. (vi) The leptoquark masses are constrained to be less than a few TeV, which should make them accessible to the LHC.

This paper is organized as follows. In Section II we discuss the model leading to two-loop neutrino mass generation and obtain the constraints placed on the oscillation parameters. The constraints from rare processes such as  $\mu^- \rightarrow e^- \gamma$  and  $\mu^- \rightarrow e^+ e^- e^-$  are presented in section III. In section IV we discuss the collider signals of leptoquarks, and in Sec. V we conclude.

## 2 Model of two-loop neutrino mass generation

In this section we present our model of two-loop neutrino mass generation, and derive restrictions on the model parameters from neutrino oscillation data. Constraints from rare processes, discussed in Sec. 3, will be used to demonstrate the viability of the model and its predictions for neutrino oscillations.

### 2.1 Model

The gauge symmetry of our model is the same as the standard model (SM),  $SU(3)_c \times SU(2)_L \times U(1)_Y$ . In addition to the SM Higgs doublet  $H(1, 2, 1/2)$ , the scalar sector consists of the following leptoquark multiplets:

$$\Omega \equiv \begin{pmatrix} \omega^{2/3} \\ \omega^{-1/3} \end{pmatrix} \sim (3, 2, 1/6), \quad \chi^{-1/3} \sim (3, 1, -1/3). \quad (3)$$

In general, addition of leptoquarks into the theory can cause baryon number ( $B$ ) violating interactions, we forbid them by assuming that  $B$  is globally conserved. The leptoquarks have the following Yukawa interactions:

$$\mathcal{L}_{\text{Yukawa}} = Y_{ij} L_i^\alpha d_j^c \Omega^\beta \epsilon_{\alpha\beta} + F_{ij} e_i^c u_j^c \chi^{-1/3} + \text{h.c.} \quad (4)$$

Here  $i, j = 1 - 3$  are family indices and  $\alpha, \beta$  are  $SU(2)_L$  indices. Note that these Yukawa couplings conserve both baryon number and lepton number ( $L$ ), as can be seen by assigning

( $B, L$ ) charges of  $(1/3, -1)$  to  $\Omega$  and  $(1/3, 1)$  to  $\chi^{-1/3}$ . The couplings  $Y'_{ij}u_i^c d_j^c \chi^*$ , allowed by the gauge symmetry are forbidden by  $B$ , and the couplings  $F'_{ij}L_i Q_j \chi^*$ , allowed by the gauge symmetry as well as  $B$  are forbidden by lepton number symmetry, which is assumed to be broken only by soft terms.<sup>3</sup> This breaking of  $L$  by two units occurs softly via a cubic term in the scalar potential:

$$V = \mu \Omega^\dagger H \chi^{-1/3} + \text{h.c.} . \quad (5)$$

The simultaneous presence of Eqs. (4) and (5) would imply that neutrino masses will be generated at the loop level, as they lead to the effective dimension 7 operator  $(Ld^c)(\overline{u^c e^c})H$  [8], once the heavy leptoquark fields are integrated out.

The Lagrangian relevant for neutrino mass generation in component form is

$$\mathcal{L}_\nu = Y_{ij}(\nu_i d_j^c \omega^{-1/3} - e_i d_j^c \omega^{2/3}) + F_{ij} e_i^c u_j^c \chi^{-1/3} - \mu(\omega^{-2/3} H^+ + \omega^{1/3} H^0) \chi^{-1/3} + \text{h.c.} \quad (6)$$

Once the neutral component of the SM Higgs doublet acquires a vacuum expectation value (VEV)  $v = 174$  GeV, the cubic term in the scalar potential will generate mixing between  $\omega^{-1/3}$  and  $\chi^{-1/3}$  leptoquarks, with a mass matrix given by

$$M_{\text{LQ}}^2 = \begin{pmatrix} m_\omega^2 & \mu v \\ \mu^* v & m_\chi^2 \end{pmatrix} . \quad (7)$$

The parameter  $\mu$  can be made real by redefining the leptoquark fields. We diagonalize this matrix to obtain the leptoquark mass eigenstates through

$$\begin{pmatrix} \omega^{-1/3} \\ \chi^{-1/3} \end{pmatrix} = \begin{pmatrix} c_\theta & s_\theta \\ -s_\theta & c_\theta \end{pmatrix} \begin{pmatrix} X_1^{-1/3} \\ X_2^{-1/3} \end{pmatrix} \quad (8)$$

where  $c_\theta = \cos \theta$ ,  $s_\theta = \sin \theta$  with the angle  $\theta$  given by

$$\tan 2\theta = \frac{2\mu v}{m_\chi^2 - m_\omega^2} . \quad (9)$$

The squared masses of  $X_{1,2}^{-1/3}$  are given by

$$M_{1,2}^2 = \frac{1}{2} \left[ m_\omega^2 + m_\chi^2 \mp \sqrt{(m_\omega^2 - m_\chi^2)^2 + 4\mu^2 v^2} \right] \quad (10)$$

with  $M_1^2 \leq M_2^2$ .

---

<sup>3</sup>The couplings  $F'_{ij}$  of course do not mediate rapid proton decay, however, their simultaneous presence with the couplings of Eq. (4) would lead to severe restrictions on  $F'_{ij}$ , since the successful  $V - A$  structure of the SM will then be drastically altered [10]. Although not essential, we prefer to set these  $F'_{ij}$  couplings to zero by  $L$  symmetry.

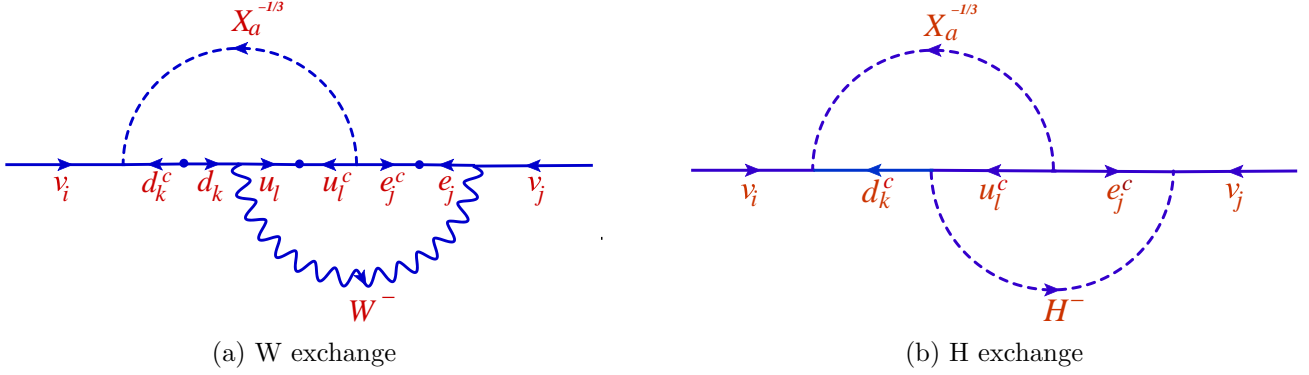


Figure 1: The two-loop diagrams contributing to neutrino mass generation.

## 2.2 Two-loop neutrino mass diagrams

Since lepton number violation occurs only when all three terms of Eq. (6) are simultaneously present, neutrino masses are generated in the model only at the two-loop level. The relevant diagrams, which involve the exchange of leptoquarks and a  $W^\pm$  boson, are shown in Fig. 1. We have evaluated these diagrams in the Feynman gauge. In this gauge, the unphysical charged Higgs boson exchange has to be kept. Interestingly, this set of charged Higgs diagrams add up to zero for the neutrino mass. The underlying reason for this result is that in the SM, both the up-type quark masses and the down-type quark masses are generated from the same Higgs doublet. Consequently the charged Higgs boson Yukawa couplings to the up-type quark has a relative minus sign compared to its Yukawa couplings to the down-type quarks, as given in the interaction Lagrangian

$$\mathcal{L}_{H^\pm} = \frac{1}{v} [\bar{u}_R M_u V d_L H^- - \bar{u}_L V M_d d_R H^- + \text{h.c.}] \quad (11)$$

Here  $V$  is the CKM matrix, and  $M_u$  and  $M_d$  are the diagonal mass matrices for the up and down quarks. When combined with Fig. 1b, this relative minus sign implies zero net contribution to the neutrino mass from the charged Higgs boson exchange. In Fig. 1b, the vertex  $u_l^c d_k^c H^+$  is a sum of two contributions, one where chirality flip occurs in the  $u_l^c$  line, and the other where it occurs in the  $d_k^c$  line. These two contributions exactly cancel, see Eq. (11).

Straightforward evaluation of the leptoquark- $W^\pm$  exchange diagrams gives the neutrino mass matrix as:

$$(M_\nu)_{ij} = \hat{m}_0 [Y_{ik}(D_d)_k(V^T)_{kl}(D_u)_l(F^\dagger)_{lj}(D_\ell)_j + (D_\ell)_i(F^*)_{il}(D_u)_l V_{lk}(D_d)_k(Y^T)_{kj}] I_{jkl} . \quad (12)$$

Here  $D_{u,d,\ell}$  are the (normalized) diagonal mass matrices for up quarks, down quarks, and charged leptons:

$$D_u = \text{diag.} \left[ \frac{m_u}{m_t}, \frac{m_c}{m_t}, 1 \right], \quad D_d = \text{diag.} \left[ \frac{m_d}{m_b}, \frac{m_s}{m_b}, 1 \right], \quad D_\ell = \text{diag.} \left[ \frac{m_e}{m_\tau}, \frac{m_\mu}{m_\tau}, 1 \right] . \quad (13)$$

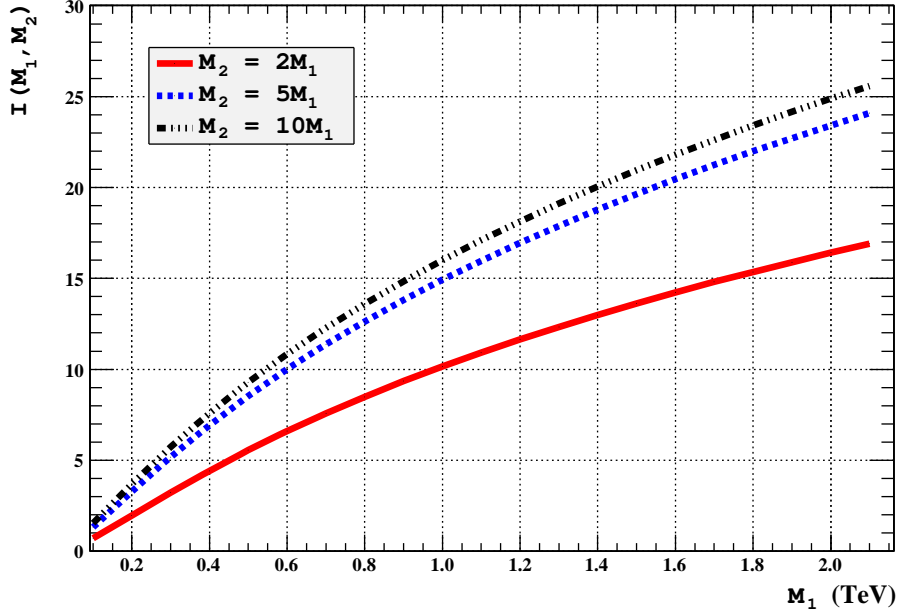


Figure 2: The exact loop integral with top quark inside the loop as a function of leptoquark masses  $M_1$  and  $M_2$ .

The overall scale  $\hat{m}_0$  is given by

$$\hat{m}_0 = \left( \frac{Cg^2 \sin 2\theta}{(16\pi^2)^2} \right) \left( \frac{m_t m_b m_\tau}{M_1^2} \right) \quad (14)$$

where  $M_1$  is the lighter of the two charge  $-1/3$  leptoquark mass and  $C = 3$  is a color factor. The dimensionless two-loop integral  $I_{jkl}$  depends on the two leptoquark masses, the  $W$  boson mass,  $m_W$ , and the up-type quark masses  $m_{u_i}$ , down-type quark masses  $m_{d_k}$  and charged lepton masses  $m_{\ell_j}$ , and is defined as

$$I_{jkl}(M_1^2, M_2^2, m_W^2) = \frac{M_1^2}{m_W^2 - m_{\ell_j}^2} \sum_{a=1,2} (-1)^a \int_0^1 dx \int_0^\infty t dt \left( \frac{1}{t + M_a^2} - \frac{1}{t + m_{d_k}^2} \right) \times \ln \left[ \frac{m_W^2(1-x) + m_{u_i}^2 x + tx(1-x)}{m_{\ell_j}^2(1-x) + m_{u_i}^2 x + tx(1-x)} \right]. \quad (15)$$

In the asymptotic limit, i.e., in the limit of  $M_{1,2}^2 \gg m_{u,d,\ell}^2, m_W^2$ , the integral  $I_{jkl}(M_1^2, M_2^2, m_W^2)$  becomes independent of the flavor indices  $j, k, l$  and takes the form

$$I_{jkl}(M_1^2, M_2^2, m_W^2) \simeq \left( 1 - \frac{M_1^2}{M_2^2} \right) \left[ 1 + \frac{\pi^2}{3} + \frac{\left( M_1^2 \ln \frac{M_2^2}{M_W^2} - M_2^2 \ln \frac{M_1^2}{M_W^2} \right)}{M_1^2 - M_2^2} + \frac{1}{2} \frac{\left( M_1^2 \ln^2 \frac{M_2^2}{m_W^2} - M_2^2 \ln^2 \frac{M_1^2}{m_W^2} \right)}{M_1^2 - M_2^2} \right]. \quad (16)$$

When the index  $l$  is not equal to 3 (corresponding to no top quark inside the loop), this asymptotic expression well approximates the exact integral. The integral  $I_{jk3}$  corresponding to

top quark inside the loop obtained numerically is shown in Fig. 2 as a function of  $M_{1,2}$ . Here we have taken the running top quark mass  $m_t(\mu = 1 \text{ TeV}) = 150 \text{ GeV}$ . It will turn out that  $I_{jk3}$  will enter into the dominant source for neutrino masses.

We now proceed to write down the neutrino mass matrix explicitly. First note that if the integral  $I_{jkl}$  in Eq. (12) is flavor universal (as happens in the asymptotic limit as given in Eq. (16)), or if  $I_{jk3}$  is the only dominant contribution,  $M_\nu$  can be written as

$$M_\nu = \hat{m}_0 \hat{I} [Y D_d V^T D_u F^\dagger D_\ell + D_\ell F^* D_u V D_d Y^T] . \quad (17)$$

where  $\hat{I}$  is the flavor universal value of  $I_{jkl}$ . Now, this equation can be expanded in power series in light fermion masses. Combining constraints from flavor changing processes, we find, to an extremely good approximation, that the neutrino mass matrix is given by

$$M_\nu \simeq m_0 \begin{pmatrix} 0 & \frac{1}{2} \frac{m_\mu}{m_\tau} xy & \frac{1}{2} y \\ \frac{1}{2} \frac{m_\mu}{m_\tau} xy & \frac{m_\mu}{m_\tau} xz & \frac{1}{2} z + \frac{1}{2} \frac{m_\mu}{m_\tau} x \\ \frac{1}{2} y & \frac{1}{2} z + \frac{1}{2} \frac{m_\mu}{m_\tau} x & 1 + w \end{pmatrix} . \quad (18)$$

Here we have used the following definition of parameters:

$$\begin{aligned} x &\equiv \frac{F_{23}^*}{F_{33}^*}, \quad y \equiv \frac{Y_{13}}{Y_{33}}, \quad z \equiv \frac{Y_{23}}{Y_{33}}, \\ w &\equiv \frac{F_{32}^* Y_{32}}{F_{33}^* Y_{33}} \left( \frac{m_c}{m_t} \right) \left( \frac{m_s}{m_b} \right) \frac{I_{jk2}}{I_{jk3}} \\ m_0 &= 2 \hat{m}_0 F_{33}^* Y_{33} I_{jk3} . \end{aligned} \quad (19)$$

As expected, the leading contributions are proportional to  $m_t m_b m_\tau$ , see the definition of  $\hat{m}_0$  in Eq. (14). One additional contribution, denoted as  $w$  in the (3,3) entry of Eq. (18), can be important, for a very restricted range of parameters. This is in spite of the additional mass suppression factors  $(m_c/m_t)(m_s/m_b)$  that appears in  $w$ , and occurs for the parameter choice  $F_{33} Y_{33} \leq 10^{-5}$  and  $M_{1,2} \sim (300 - 500) \text{ GeV}$ . The Yukawa coupling combination  $F_{32} Y_{32}$  appearing in  $w$  is allowed to be order one, these couplings do not lead to excessive flavor violating processes even when the leptoquarks are light. ( $F_{32}$  couples  $\tau_R$  to  $c_R$ , and  $Y_{32}$  couples  $L_3$  to  $s_R$ , both of which are found to be rather un-constrained.) Contributions not shown in Eq. (18) have magnitudes  $\ll 0.01 \text{ eV}$ , because of mass suppression factors and the constraints on the Yukawa couplings arising from rare processes mediated by the leptoquarks.

We shall consider the case  $w \ll 1$  for the most part of our analysis, but we shall also examine the special case where  $w \gg 1$ , which will be realized when the coupling  $F_{33}$  takes anomalously small value and the leptoquark mass is less than about 500 GeV.

The zero in the (1,1) entry of Eq. (18) is highly suppressed. We find, using the lowest non-vanishing contribution from Eq. (17) for this entry to be

$$(M_\nu)_{11} \simeq y \left( \frac{F_{13}^*}{F_{33}^*} \right) \left( \frac{m_e}{m_\tau} \right) m_0 . \quad (20)$$

Now, unless  $(F_{13}^*/F_{33}^*) = (F_{13}^*/F_{23}^*)x$  takes values as large as  $m_\tau/m_e \sim 4000$ , this entry will be negligible for neutrino masses. That possibility is however inconsistent with an acceptable fit to neutrino data on the one hand, and flavor violating constraints on the other. To see this, let us note that a good fit to neutrino data, discussed in more detail later in this section, requires  $|Y_{33}| \sim |Y_{23}| \sim |Y_{13}|$  and  $x = |F_{23}|/|F_{33}| \sim m_\tau/m_\mu \sim 16$ . Further, the leptoquark mass should not exceed about 10 TeV, or else the neutrino mass  $m_3$  will be smaller than 0.05 eV, which would be inconsistent with the atmospheric oscillation data. For the same reason,  $F_{33} \ll 1$ , while allowed, would require the leptoquark mass to be much below a TeV. Then flavor violation constraints become important.  $\mu - e$  conversion in nuclei sets an upper limit on the products  $|F_{13}F_{23}| < 10^{-4}$  and  $|Y_{13}Y_{23}| < 10^{-4}$  corresponding to a leptoquark mass of 300 GeV. When these limits are combined with the need to obtain the right magnitude for  $m_3$ , we see that  $|F_{23}|$  cannot be smaller than  $10^{-2}$ . Consequently the (1,1) entry of  $M_\nu$ , given in Eq. (20), is much smaller than 0.01 eV. This of course means that contributions to neutrinoless double beta decay from light neutrino exchange is negligible. See however, other contributions to this process via the exchange of a leptoquark and  $W$  boson in Fig. 10 discussed later, which turns out to be significant.

The other remarkable feature of the mass matrix in Eq. (17) is that, although it may not be obvious from its form,  $M_\nu$  has nearly zero determinant when  $w \ll 1$ . This would imply that one of the neutrinos is essentially massless in the model for most of the parameter space. This can be seen by observing that only the top quark mass, and not the  $c$  and  $u$  quark masses, has entered into  $M_\nu$  when  $w$  is set to zero. In this case, each of the two terms in Eq. (17) has rank one, and the sum of the two terms has rank two, leaving the determinant to be zero. The first non-zero entry to the determinant in our expansion is found to be

$$\begin{aligned} \text{Det}(M_\nu) \simeq & \frac{y}{4} m_0^3 \left(\frac{m_c}{m_t}\right) \left(\frac{m_s}{m_b}\right) \left(\frac{m_\mu}{m_\tau}\right) \left(\frac{I_{jk2}}{I_{jk3}}\right) \left(x \frac{F_{32}^*}{F_{33}^*} - \frac{F_{22}^*}{F_{33}^*}\right) \\ & \times \left[ \left(y \frac{Y_{22}}{Y_{33}} - z \frac{Y_{12}}{Y_{33}}\right) + x \left(\frac{m_\mu}{m_\tau}\right) \left(\frac{Y_{12}}{Y_{33}} - y \frac{Y_{32}}{Y_{33}}\right) \right]. \end{aligned} \quad (21)$$

Again, with  $|x| \sim m_\tau/m_\mu \sim 16$ ,  $|y| \sim 1$ , and  $w \ll 1$  (or equivalently  $Y_{32}F_{32}^* \ll 10^4 Y_{33}F_{33}^*$ ), the determinant will be much less than  $(0.01 \text{ eV})^3$  and thus  $m_1 \simeq 0$  to a high degree of accuracy. Note that  $F_{33}^*$  cannot be less than  $10^{-3}$ , or else the neutrino mass scale will be too small.

### 2.3 Predictions for neutrino oscillations when $w \ll 1$

We turn now to the predictions of the model when  $w \ll 1$ , which is realized in much of the parameter space. Since  $M_\nu$  in Eq. (18) has only four (complex) parameters, there are two predictions for neutrino masses and mixings. These are summarized below:

$$m_1 \simeq 0, \quad \tan^2 \theta_{13} \simeq \frac{m_2}{m_3} \sin^2 \theta_{12}. \quad (22)$$



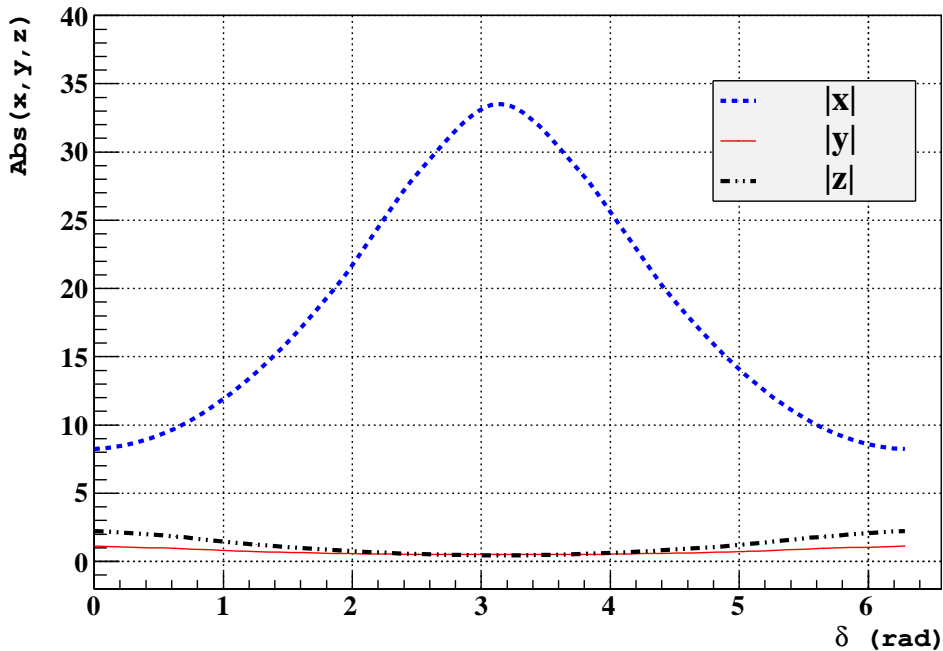


Figure 3: The absolute values of  $x$ ,  $y$ ,  $z$

Here we have used the standard parametrization of the PMNS matrix. Furthermore, the two Majorana phases  $\alpha$  and  $\beta$  (the phases of masses  $m_1$  and  $m_2$  respectively) are given by

$$\beta \simeq 2\delta + \pi, \quad \alpha \simeq 0, \quad (23)$$

with  $\alpha \simeq 0$  being a consequence of  $m_1 \simeq 0$ . These predictions have been obtained in the context of textures before (see Ref. [12] and the references therein). Here we have derived them without resorting to textures.

To check the consistency of these predictions, we keep  $\Delta m_{\text{solar}}^2 = 7.65 \times 10^{-5} \text{ eV}^2$ ,  $\Delta m_{\text{atm}}^2 = 2.40 \times 10^{-3} \text{ eV}^2$  at their central values [13], and then vary  $\sin^2 \theta_{12} = 0.304_{-0.016}^{+0.022}$  in its allowed range. This gives from Eq. (22)

$$\sin^2 \theta_{13} = \{0.051, 0.049, 0.046, 0.044\}, \quad (24)$$

where the numbers correspond to the central value, and (1, 2, 3)  $\sigma$  deviation in  $\sin^2 \theta_{12}$ . This should be compared with the limit  $\sin^2 \theta_{13} \leq (0.040, 0.056)$ , at the (2, 3) $\sigma$  level [13]. We see broad agreement, although  $\sin^2 \theta_{13}$  should be very close to the current limit.

We can infer the values of  $(x, y, z)$  in Eq. (18) from neutrino data. For this purpose we use the central values from neutrino data:  $\Delta m_{\text{solar}}^2 = 7.65 \times 10^{-5} \text{ eV}^2$ ,  $\Delta m_{\text{atm}}^2 = 2.40 \times 10^{-3} \text{ eV}^2$ , along with  $\sin^2 \theta_{23} = 0.50$ ,  $\sin^2 \theta_{12} = 0.304$ , and  $\sin^2 \theta_{13} = 0.051$  [13]. We obtain

$$x = \frac{12.21 - 4.17e^{i\delta}}{0.726 + 0.248e^{i\delta}}, \quad y = \frac{-0.112e^{i\delta}(2.927 + e^{i\delta})}{-0.473 + 0.018e^{i\delta} + 0.062e^{2i\delta}}, \quad z = \frac{0.473 + 0.342e^{i\delta} + 0.062e^{2i\delta}}{0.473 - 0.018e^{i\delta} - 0.062e^{2i\delta}}. \quad (25)$$

The absolute values of  $x$ ,  $y$ ,  $z$  are given in Fig. 3. We see that  $|x| \gg 1$  and  $|y|, |z| \sim 1$ . These values will directly affect the branching ratios of the leptoquarks, making a strong connection between collider physics and neutrino physics.

## 2.4 A special case with $w \gg 1$

It is interesting to see the constraints on the model when  $w \gg 1$ . This occurs for a small range of parameters when the leptoquark mass is less than about 500 GeV, and when  $|F_{33}Y_{33}| \ll 10^{-5}$ . The latter condition can be satisfied when either  $|F_{33}|$  or  $|Y_{33}|$  is much smaller than  $10^{-5}$ . Both of these couplings cannot be simultaneously very small, or else the (2,3) entry of  $M_\nu$  will become unacceptably small.

When  $F_{33} \rightarrow 0$ , we have the condition  $(M_\nu)_{13} \simeq 0$ , see Eq. (18). Since  $(M_\nu)_{11} \simeq 0$  in this case we reproduce a well known texture model [16, 17]. This limit of our model leads to the following predictions for  $\sin^2 \theta_{13}$  and the phase parameters:

$$\sin^2 \theta_{13} \simeq \frac{|\Delta m_{\text{solar}}^2|/|\Delta m_{\text{atm}}^2|}{|\cot^2 \theta_{12} - e^{i2(\alpha-\beta)} \tan^2 \theta_{12}|}, \quad (26)$$

$$\tan 2(\beta + \delta) \simeq \frac{\tan^2 \theta_{12} \sin 2(\alpha - \beta)}{\cot^2 \theta_{12} - \tan^2 \theta_{12} \cos 2(\alpha - \beta)}. \quad (27)$$

This gives  $0.012 \leq \sin^2 \theta_{13} \leq 0.017$ , which is within reach of the next generation long baseline neutrino oscillation experiments. This case requires the leptoquarks to be lighter than about 500 GeV, which are within reach of the LHC.

## 2.5 The case of $w \sim 1$

For the case when  $w \sim 1$ , there are no restrictions on the neutrino oscillation parameters, except the one arising from the vanishing of the (1,1) entry of  $M_\nu$ . This relation can be taken to be a prediction for  $m_1$ , and an additional relation for the phase parameters. These are given by

$$\begin{aligned} \tan^2 \theta_{13} &\simeq \frac{m_2}{m_3} \sin^2 \theta_{12} \left| 1 + \frac{m_1}{m_2} \cot^2 \theta_{12} e^{i(\alpha-\beta)} \right|, \\ 2\delta &\simeq \beta - \pi - \cot^{-1} \left[ \frac{1 + a \cos(\beta - \alpha)}{a \sin(\beta - \alpha)} \right], \end{aligned} \quad (28)$$

where  $a \equiv \frac{m_1}{m_2} \cot^2 \theta_{12}$ . In this scenario  $\theta_{13}$  can take any value between zero and its current experimental upper limit. For  $w \sim 1$ , the leptoquark mass cannot exceed about 500 GeV, so this scenario is testable at the LHC.

## 2.6 Limit on the parameter $\mu$

There are certain restrictions on the parameter  $\mu$  that enters in the neutrino mass Lagrangian of Eq. (6). It is this term that is responsible for the mixing of  $\omega^{-1/3}$  with  $\chi^{-1/3}$ . Since the  $SU(2)_L$

partner of  $\omega^{-1/3}$  does not mix with any other field, the  $\mu$  term will induce new contributions to the electroweak  $\rho$  parameter (or equivalently the  $T$  parameter). This is because mixing via the  $\mu$  term splits the masses of the  $SU(2)_L$  doublet members. This mass-splitting must obey [11]

$$\frac{C}{3}(\Delta M)^2 \leq (57 \text{ GeV})^2, \quad (29)$$

where  $C = 3$  for leptoquarks. In our model, there apart from the  $\mu$  term, there is a quartic scalar coupling,  $V \supset \kappa |(\Omega^\dagger H)|^2$ , which contributes to the  $\omega^{-1/3}$  mass, and not to the  $\omega^{2/3}$  mass, causing a further splitting. The parameter  $(\Delta M)^2$  in Eq. (29) is given by

$$\Delta M \simeq \frac{\kappa v^2 + M_1^2 - m_\omega^2}{2M_1}, \quad (30)$$

where we have assumed that the two states are nearly degenerate. The two-loop induced neutrino mass is maximized when the mixing parameter  $\sin 2\theta = 1$ . For this choice, one has the relations  $M_{1,2}^2 = m_\omega^2 \mp \mu v$ . When the leptoquark mass is well above 200 GeV, the contribution  $\kappa v^2$  in Eq. (30), which is at most of order  $(200 \text{ GeV})^2$ , can be neglected in relation to the  $\mu v$  term. In this case we obtain from Eq. (29) an upper limit on  $\mu$ :  $\mu \leq 0.65 M_1$ . We shall use this constraint in deriving an upper limit on the leptoquark mass.

There are other reasons why  $\mu$  cannot be arbitrarily large: the positivity of leptoquark squared mass (needed for color conservation) and the perturbativity of the theory. The first of these conditions implies, from Eq. (10), that

$$\mu \leq \frac{m_\omega m_\chi}{v}. \quad (31)$$

The second constraint emerges because  $\mu$  induces negative quartic couplings for the three fields  $\chi^{1/3}$ ,  $\omega^{1/3}$  and  $H^0$ . These induced couplings cannot exceed the corresponding tree-level quartic couplings which can at most be of order one. Otherwise the theory would be non-perturbative, or electric charge and color would break in the minimum of the theory. We parameterize the effective quartic couplings of the three fields as

$$-\mathcal{L}_{\text{eff}} = \lambda_{\text{eff}} (H^{0*} H^0)^2 + \lambda'_{\text{eff}} (\chi^* \chi)^2 + \lambda''_{\text{eff}} (\omega^* \omega)^2, \quad (32)$$

with  $H^0 = h/\sqrt{2}$ . The 1-loop correction to these quartic couplings are shown in Fig. 4.<sup>4</sup> By evaluating these diagrams we obtain for the effective couplings,

$$\begin{aligned} \lambda_{\text{eff}} &= -\frac{3}{32\pi^2} \frac{\mu^4}{(m_\chi^2 - m_\omega^2)^2} \left[ \frac{m_\chi^2 + m_\omega^2}{m_\chi^2 - m_\omega^2} \ln \frac{m_\chi^2}{m_\omega^2} - 2 \right] \\ \lambda'_{\text{eff}} &= -\frac{1}{128\pi^2} \frac{\mu^4}{(m_\chi^2 - m_h^2)^2} \left[ \frac{m_\chi^2 + m_h^2}{m_\chi^2 - m_h^2} \ln \frac{m_\chi^2}{m_h^2} - 2 \right] \\ \lambda''_{\text{eff}} &= -\frac{1}{128\pi^2} \frac{\mu^4}{(m_\omega^2 - m_h^2)^2} \left[ \frac{m_\omega^2 + m_h^2}{m_\omega^2 - m_h^2} \ln \frac{m_\omega^2}{m_h^2} - 2 \right], \end{aligned} \quad (33)$$

---

<sup>4</sup>For the  $h^4$  term, there is a similar diagram generated by the SM  $(H^\dagger H)^2$  quartic coupling. But here we focus on the diagrams generated by the  $\mu$  term.

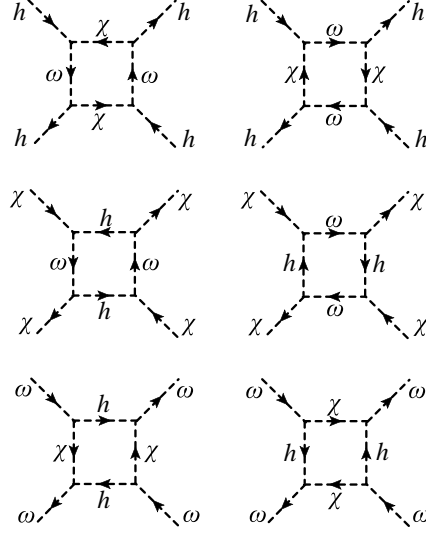


Figure 4: The diagrams leading to the quartic couplings correction generated by  $\mu$ .

where the factor in  $\lambda_{\text{eff}}$  is a color factor. Since these effective couplings are negative, they must be smaller in magnitude compared to the corresponding tree level ones, otherwise the potential would become unbounded, suggesting instability of the vacuum. By demanding all these induced couplings to be less than one, so that the theory is perturbative with a stable vacuum, one can derive limits of  $\mu$ . Of course, if the limit derived from Eq. (31) turns out to be more stringent, that will supersede the present limits.

For illustration, we consider few examples simplified cases.

- $m_h \approx m_\omega \ll m_\chi$ . For  $m_h = m_\omega = 200$  GeV and  $m_\chi = 1$  TeV, the bound from Eq. (31) gives a more stringent limit, i.e.  $\mu < 1.1$  TeV. For  $m_\chi = 2$  TeV and the other masses the same as above, the more stringent limit comes from the  $\lambda_{\text{eff}}$ , viz.,  $\mu < 1.9$  TeV.
- $m_h \ll m_\omega \neq m_\chi$ : In this case

$$\mu < m \left( \frac{64\pi^2}{\ln \frac{m}{m_h} - 1} \right)^{1/4}, \quad (34)$$

where  $m$  is the smallest of  $m_\omega$  and  $m_\chi$ . For example, if  $m_\omega = 1$  TeV,  $m_\chi = 2$  TeV, and  $m_h = 200$  GeV,  $\mu < 5.7$  TeV.

- $m_h \ll m_\omega \approx m_\chi$ : In this case

$$\mu < m_\chi (64\pi^2/\xi)^{1/4}, \quad (35)$$

where  $\xi = \max \{1, \ln \frac{m_\chi}{m_h} - 1\}$ . The choice of  $\xi$  depends upon the value of  $m_\omega$  and  $m_\chi$ . For example, if  $m_\omega = m_\chi = 1$  TeV and  $m_h = 200$  GeV, one uses  $\xi = 1$ , so  $\mu < 5$  TeV. On the other hand, if  $m_\omega = m_\chi = 2$  TeV and  $m_h = 200$  GeV, one uses  $\xi = \left( \ln \frac{m_\chi}{m_h} - 1 \right)$ , so  $\mu < 9.4$  TeV.

## 2.7 Limit on leptoquark masses

The scaling of the neutrino mass with the LQ mass goes as  $(m_\nu \sim m_t m_b m_\tau \mu v)/M_1^4$ . Since our neutrino mass matrix has a normal hierarchy structure, the neutrino mass scale  $m_0$  should be around 0.02 eV. We shall assume that all the Yukawa couplings are bounded by 1, a requirement for perturbative treatment of the problem. As we have seen, a fit to the neutrino oscillation data requires  $F_{33}/F_{23} \sim m_\mu/m_\tau \sim 1/16$ . The maximum value of  $m_0$  is realized for  $\sin 2\theta = 1$ , corresponding to largest allowed LQ mass. From these considerations we arrive at a limit on the LQ mass of 12 TeV. If the leptoquarks are in the multi-TeV range, all three members should be nearly degenerate, from the requirement of  $\sin 2\theta \approx 1$  and the  $\rho$  parameter constraint. A slightly better limit can be derived on their masses from the rare process  $\mu - e$  conversion in nuclei (see the next section for details). From the experimental limit on this process, one can derive the upper limit on  $|Y_{13}^* Y_{23}|$  as a function of  $\omega^{2/3}$  mass. Since neutrino mass fitting requires  $Y_{i3}$  to be in the same order for  $i = 1 - 3$ , one can also determine an upper limit on  $Y_{33}$ . Combining all of these, we obtain an upper limit of 10 TeV on  $M_1$ .

There are lower limits on leptoquark mass from the Tevatron where they could be pair produced. The D0 and CDF experiments [14] have obtained limits on the second and the third generation leptoquarks of 316 GeV and 245 GeV respectively [14, 15]. Since those experiments look for b-jets and missing energy, these bounds are strictly applicable for leptoquarks coupled to neutrinos. In our case,  $\omega^{-1/3}$  and  $\chi^{-1/3}$  have direct couplings to the neutrinos (the latter from mixing) for which the quoted limits apply. As for  $\omega^{2/3}$ , being a member of the same  $SU(2)_L$  doublet as  $\omega^{-1/3}$ , it should be nearly degenerate with  $\omega^{-1/3}$ , and thus the limits of Ref. [14] should apply to  $\omega^{2/3}$  as well.

## 3 Constraints from rare processes

Since this model features lepton flavor (as well as total lepton number) violation, it is important to see how its parameters are constrained by the experimental data, especially those arising from rare decay processes that are forbidden in the SM. Here we derive a variety of limits on the couplings  $Y_{ij}$  and  $F_{ij}$  as functions of the LQ masses. These limits should be (and have been) satisfied in the neutrino fits. The processes we shall consider are  $\mu^- \rightarrow e^- \gamma$ ,  $\mu^- \rightarrow e^+ e^- e^-$ ,  $\mu - e$  conversion in the nuclei,  $\tau^- \rightarrow e^- \eta$ ,  $\tau^- \rightarrow \mu^- \eta$ ,  $B_{s,d} - \bar{B}_{s,d}$  mixing,  $K - \bar{K}$  mixing,  $D - \bar{D}$  mixing,  $D_s^\pm \rightarrow \ell^\pm \nu$  decay, muon  $g - 2$ ,  $\pi^+ \rightarrow \mu^+ \bar{\nu}_e$  decay, and neutrinoless double beta decay. The expected rates for several of these processes are found to be in the interesting range for the next generation of experiments.

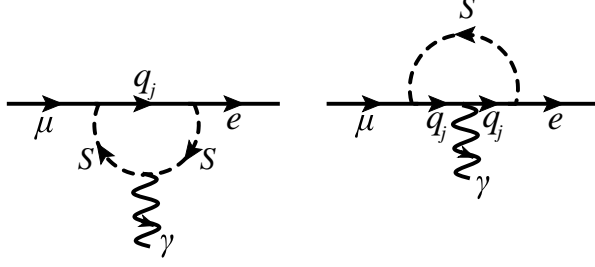


Figure 5: The diagrams leading to  $\mu \rightarrow e\gamma$ .  $q_j$  and  $S$  represent  $d_j$  ( $u_j^c$ ) quarks and  $\omega^{2/3}$  ( $\chi^{1/3}$ ) respectively.

### 3.1 $\mu^- \rightarrow e^- \gamma$

The rare decay  $\mu^- \rightarrow e^- \gamma$  arises from a one-loop diagram. In the limit of  $m_e = 0$ , there are only three diagrams for this decay shown in Fig. 5. In general, the amplitude for this decay process can be written as [18]

$$\mathcal{M} = -e \frac{i q_\nu}{m_\mu} \bar{u}(p_e) \sigma^{\mu\nu} (f_{M1} + f_{E1} \gamma_5) u(p_\mu) \epsilon_\mu(q) \quad (36)$$

where  $m_\mu$  is the muon mass,  $q \equiv p_\mu - p_e$  is the photon momentum, and  $\epsilon_\mu$  is the photon polarization vector. The effective couplings  $f_{M1}$  and  $f_{E1}$  are found to be (repeated indices implies summation)

$$\begin{aligned} f_{E1} &= \frac{3m_\mu^2}{32\pi^2} \left( \frac{Y_{1j}^* Y_{2j}}{m_\omega^2} F_3(x_{d_j}) - \frac{F_{1j} F_{2j}^*}{m_\chi^2} F_4(x_{u_j}) \right), \\ f_{M1} &= \frac{3m_\mu^2}{32\pi^2} \left( \frac{Y_{1j}^* Y_{2j}}{m_\omega^2} F_3(x_{d_j}) + \frac{F_{1j} F_{2j}^*}{m_\chi^2} F_4(x_{u_j}) \right), \end{aligned} \quad (37)$$

where  $x_{d_j} \equiv m_{d_j}^2/m_\omega^2$ ,  $x_{u_j} \equiv m_{u_j}^2/m_\chi^2$ ;  $m_{u_j}$  and  $m_{d_j}$  are the  $j$ -th generation of up- and down-type quark masses respectively;  $m_\omega$  and  $m_\chi$  are  $\omega^{2/3}$  and  $\chi^{1/3}$  masses respectively; and  $F_3(x)$  and  $F_4(x)$  are the dimensionless functions given by [19, 20]

$$\begin{aligned} F_3(x) &= -\frac{x}{12} \frac{(1-x)(5+x) + 2(2x+1) \ln x}{(1-x)^4}, \\ F_4(x) &= -\frac{1}{12} \frac{(1-x)(5x+1) + 2x(2+x) \ln x}{(1-x)^4}. \end{aligned} \quad (38)$$

These expressions assume that the leptoquark mixing angle  $\theta$  (see Eq. (9)) is zero. For non-zero  $\theta$ , one can make the following replacement:

$$\frac{1}{m_\chi^2} \rightarrow \sum_{a=1}^2 \frac{\zeta_a}{M_a^2}, \quad (39)$$

where  $\zeta_1 = \sin^2 \theta$ ,  $\zeta_2 = \cos^2 \theta$ , and  $M_a$  are defined in Eq. (10).

Process	BR	Constraint
$\mu \rightarrow e\gamma$	$< 1.2 \times 10^{-11}$	$\frac{ F_3(x_b)Y_{13}^*Y_{23} ^2}{m_\omega^4} + \frac{ \frac{1}{12}F_{11}F_{21}^* + \frac{1}{12}F_{12}F_{22}^* + F_4(x_t)F_{13}F_{23}^* ^2}{m_\chi^4} < \frac{3.1 \times 10^{-19}}{\text{GeV}^4}$
$\tau \rightarrow e\gamma$	$< 1.1 \times 10^{-7}$	$\frac{ F_3(x_b)Y_{13}^*Y_{33} ^2}{m_\omega^4} + \frac{ \frac{1}{12}F_{11}F_{31}^* + \frac{1}{12}F_{12}F_{32}^* + F_4(x_t)F_{13}F_{33}^* ^2}{m_\chi^4} < \frac{1.6 \times 10^{-14}}{\text{GeV}^4}$
$\tau \rightarrow \mu\gamma$	$< 4.5 \times 10^{-8}$	$\frac{ F_3(x_b)Y_{23}^*Y_{33} ^2}{m_\omega^4} + \frac{ \frac{1}{12}F_{21}F_{31}^* + \frac{1}{12}F_{22}F_{32}^* + F_4(x_t)F_{23}F_{33}^* ^2}{m_\chi^4} < \frac{6.7 \times 10^{-15}}{\text{GeV}^4}$

Table 1: The constraints from  $\ell_i \rightarrow \ell_j\gamma$ .

It is an excellent approximation to set the first and second generation quark masses to zero. The branching ratio for this decay is found to be

$$\text{BR}(\mu^- \rightarrow e^- \gamma) = \frac{27\alpha}{16\pi G_F^2} \left( \frac{|F_3(x_b)Y_{13}^*Y_{23}|^2}{m_\omega^4} + \frac{|\frac{1}{12}F_{11}F_{21}^* + \frac{1}{12}F_{12}F_{22}^* + F_4(x_t)F_{13}^*F_{23}|^2}{m_\chi^4} \right), \quad (40)$$

where  $\alpha = e^2/4\pi$  is the fine structure constant. Constraints from other  $\ell_i \rightarrow \ell_j\gamma$  processes are presented in Table 1, where we have used the approximation  $m_{\ell_j} = 0$ .

An interesting feature of this analysis is that the  $Y_{ij}$  couplings are only weakly constrained from these processes. This is owing to a GIM-like cancelation for the amplitude of this process from the two diagrams (Fig. 5). In the limit of down-type quark mass being zero, the two graphs exactly cancel. This cancelation occurs because the charge of the internal leptoquark ( $2/3$ ) is twice as large and opposite in sign compared to the charge of the internal down quark ( $-1/3$ ). The amplitude of the graph where the photon is emitted from the scalar line is twice smaller compared to the one where the photon is emitted from the fermion line, leading to the cancelation. The non-canceling contribution is suppressed by a factor  $m_b^2/m_\omega^2$  in the amplitude, which weakens the limit.

### 3.2 $\mu^- \rightarrow e^+ e^- e^-$

These processes also occur at the one-loop level in our model (see Fig. 6). Here, there exist photon,  $Z$ -boson, and the SM Higgs-boson exchange diagrams, as well as box diagrams. The SM Higgs diagrams are suppressed by the electron mass, and thus highly suppressed and therefore ignored. Therefore, only the photon,  $Z$ -boson, and the box diagrams will be evaluated.

In the case of photon exchange, because the photon is now off-shell, and with the electron

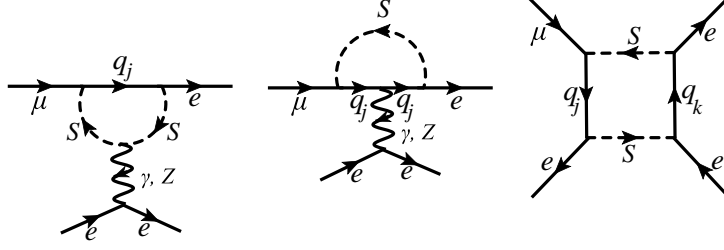


Figure 6: The diagrams leading to  $\mu \rightarrow 3e$ .  $q_j$  and  $S$  represent  $d_j$  ( $u_j^c$ ) quarks and  $\omega^{2/3}$  ( $\chi^{1/3}$ ) respectively.

mass set to zero, the amplitude is given by

$$\begin{aligned}
\mathcal{M}_\gamma &= \frac{e^2}{m_\mu^2} [\bar{u}(p_{e1})\gamma^\mu (f_{E0} + f_{M0}\gamma_5)u(p_\mu)] [\bar{u}(p_{e2})\gamma_\mu v(p_{e3})] \\
&+ e^2 \frac{i q_\nu}{m_\mu q^2} [\bar{u}(p_{e1})\sigma^{\mu\nu} (f_{M1} + f_{E1}\gamma_5)u(p_\mu)] [\bar{u}(p_{e2})\gamma_\mu v(p_{e3})] \\
&- (p_{e1} \leftrightarrow p_{e2}),
\end{aligned} \tag{41}$$

where  $q \equiv p_\mu - p_{e1}$ .  $p_\mu$  and  $p_{ei}$  are the incoming muon and outgoing electron momenta respectively. The couplings  $f_{E0}$  and  $f_{M0}$  are found to be

$$\begin{aligned}
f_{E0} &= \frac{3m_\mu^2}{32\pi^2} \left( \frac{Y_{1j}^* Y_{2j}}{m_\omega^2} g_j + \frac{F_{1j} F_{2j}^*}{m_\chi^2} h_j \right), \\
f_{M0} &= -\frac{3m_\mu^2}{32\pi^2} \left( \frac{Y_{1j}^* Y_{2j}}{m_\omega^2} g_j - \frac{F_{1j} F_{2j}^*}{m_\chi^2} h_j \right),
\end{aligned} \tag{42}$$

where  $g_{1,2} = \frac{1}{27}(2 - 3 \ln \frac{q^2}{m_\omega^2})$ ,  $h_{1,2} = \frac{1}{54}(5 - 12 \ln \frac{q^2}{m_\chi^2})$ ,  $g_3 = F_1(x_b)$ , and  $h_3 = F_2(x_t)$ . The dimensionless functions  $F_1(x)$  and  $F_2(x)$  are given by [20]

$$\begin{aligned}
F_1(x) &= \frac{-4 + 9x - 5x^3 + 2(2x^3 + 3x - 2) \ln x}{36(1-x)^4}, \\
F_2(x) &= \frac{(x-1)(10 + x(x-17)) + 2(x^3 + 6x - 4) \ln x}{36(1-x)^4}.
\end{aligned} \tag{43}$$

For the  $Z$  boson exchange diagram, the leading contribution after ignoring terms suppressed by  $m_\mu^2/M^2$ , with  $M$  being leptoquarks mass, is

$$\begin{aligned}
\mathcal{M}_Z &= \frac{G_F}{\sqrt{2}} [\eta_L \bar{u}_L(p_{e1})\gamma^\mu u_L(p_\mu) + \eta_R \bar{u}_R(p_{e1})\gamma^\mu u_R(p_\mu)] \\
&\times [\bar{u}(p_{e2})\gamma_\mu (g_V^e - g_A^e \gamma_5)v(p_{e3})] \\
&- (p_{e1} \leftrightarrow p_{e2}),
\end{aligned} \tag{44}$$

where  $g_V^e = -\frac{1}{4} + \sin^2 \theta_W$  and  $g_A^e = -\frac{1}{4}$ . Since we set the first and second generation quark masses to zero (which is a good approximation), the effective couplings,  $\eta_L$  and  $\eta_R$ , therefore, is



given by

$$\begin{aligned}\eta_L &= \frac{3}{2\pi^2} Y_{13}^* Y_{23} F_5(x_b), \\ \eta_R &= \frac{3}{2\pi^2} F_{13} F_{23}^* F_5(x_t),\end{aligned}\tag{45}$$

with

$$F_5(x) = -\frac{x}{2} \frac{1-x+\ln x}{(1-x)^2}.\tag{46}$$

For the box diagrams, the amplitude can be written as

$$\begin{aligned}\mathcal{M}_{\text{box}} &= \frac{3}{64\pi^2 m_\omega^2} (YY^\dagger)_{11} (YY^\dagger)_{21} [\overline{u}_L(p_{e1})\gamma^\mu u_L(p_\mu)] [\overline{u}_L(p_{e2})\gamma_\mu v_L(p_{e3})] \\ &\quad + \frac{3}{64\pi^2 m_\chi^2} (FF^\dagger)_{11} (FF^\dagger)_{12} [\overline{u}_R(p_{e1})\gamma^\mu u_R(p_\mu)] [\overline{u}_R(p_{e2})\gamma_\mu v_R(p_{e3})] \\ &\quad - (p_{e1} \leftrightarrow p_{e2}).\end{aligned}\tag{47}$$

Here we have set all the quark masses to zero.

We now proceed to the calculation of the total amplitude. In the loop integral functions,  $F_1\dots F_5$ , since the  $Y_{ij}$  couplings are not constrained by  $\mu^- \rightarrow e^- \gamma$ , one needs to include all the diagrams mediated by  $\omega^{2/3}$  boson, since the  $Y_{ij}$  couplings may be of order one. However, since the  $Z$ -boson exchange contribution is suppressed by the the bottom quark mass, it can safely be ignored. On the other hand, the  $Z$  exchange is significant for  $\chi^{1/3}$  mediated process with the top quark inside the loop. The electron mass has to be included in the calculation in order to avoid infrared singularity. The branching ratio is found to be

$$\text{BR}(\mu^- \rightarrow e^+ e^- e^-) = \left( \frac{3\sqrt{2}}{32\pi^2 G_F} \right)^2 \left( \frac{C_{jk}^L Y_{1j}^* Y_{2j} Y_{1k} Y_{2k}^*}{m_\omega^4} + \frac{C_{jk}^R F_{1j}^* F_{2j} F_{1k} F_{2k}^*}{m_\chi^4} \right),\tag{48}$$

where we have introduced Hermitian parameters  $C_{jk}^{L,R}$ , given by

$$\begin{aligned}
C_{jk}^L &= \begin{cases} \frac{1}{7776} \left[ 72e^4 \ln^2 \frac{m_\mu^2}{m_\omega^2} - 108 (3e^4 + 2e^2 (YY^\dagger)_{11}) \ln \frac{m_\mu^2}{m_\omega^2} \right. \\ \left. + (449 + 68\pi^2) e^4 + 486e^2 (YY^\dagger)_{11} + 243 (YY^\dagger)_{11}^2 \right], \text{ for } j, k = 1, 2; \\ \\ \frac{1}{288} \left[ 54e^4 F_1(x_b) - 4e^2 (6e^2 F_1(x_b) + (YY^\dagger)_{11}) \left( \ln \frac{m_\mu^2}{m_\omega^2} + i\pi \right) + 36e^2 (YY^\dagger)_{11} F_1(x_b) \right. \\ \left. + 9e^2 (YY^\dagger)_{11} + 9 (YY^\dagger)_{11}^2 \right], \text{ for } j = 1, 2 \text{ and } k = 3; \\ \\ \frac{1}{32} \left[ 24e^4 F_1^2(x_b) + 8e^2 (YY^\dagger)_{11} F_1(x_b) + (YY^\dagger)_{11}^2 \right], \text{ for } j = k = 3; \end{cases} \\
C_{jk}^R &= \begin{cases} \frac{e^4}{7776} \left( 288 \ln^2 \frac{m_\mu^2}{m_\chi^2} - 1584 \ln \frac{m_\mu^2}{m_\chi^2} + 108 \ln \frac{m_\mu^2}{m_e^2} + 272\pi^2 + 2759 \right) \\ + \frac{e^2}{72} (FF^\dagger)_{11} \left( 11 - 4 \ln \frac{m_\mu^2}{m_\chi^2} \right) + \frac{1}{32} (FF^\dagger)_{11}^2, \text{ for } j, k = 1, 2; \\ \\ \frac{e^4}{24} \left[ 11F_2(x_t) - 29F_4(x_t) - 4F_4(x_t) \ln \frac{m_\mu^2}{m_e^2} - 4(F_2(x_t) - 2F_4(x_t)) \left( \ln \frac{m_\mu^2}{m_\chi^2} + i\pi \right) \right] \\ + \frac{e^2}{144} \left[ 4\sqrt{2}(6 \sin^2 \theta_W - 1) G_F m_\chi^2 F_5(x_t) \left( -4 \ln \frac{m_\mu^2}{m_\chi^2} - i4\pi + 11 \right) \right. \\ \left. + (FF^\dagger)_{11} \left( 18F_2(x_t) - 36F_4(x_t) - 4 \ln \frac{m_\mu^2}{m_\chi^2} - i4\pi + 11 \right) \right] \\ + \frac{1}{32} (FF^\dagger)_{11} \left[ 16\sqrt{2} \sin^2 \theta_W G_F m_\chi^2 F_5(x_t) + (FF^\dagger)_{11} \right], \text{ for } j = 1, 2 \text{ and } k = 3; \\ \\ e^4 \left[ \frac{3}{4} F_2^2(x_t) - 3F_2(x_t)F_4(x_t) + 2F_4^2(x_t) \left( \ln \frac{m_\mu^2}{m_e^2} - \frac{11}{4} \right) \right] \\ + \frac{e^2}{4} [F_2(x_t) - 2F_4(x_t)] \left[ 4\sqrt{2}(6 \sin^2 \theta_W - 1) G_F m_\chi^2 F_5(x_t) + (FF^\dagger)_{11} \right] \\ + 2(1 - 4 \sin^2 \theta_W + 12 \sin^4 \theta_W) G_F^2 m_\chi^4 F_5^2(x_t) \\ + \sqrt{2} (FF^\dagger)_{11} \sin^2 \theta_W G_F m_\chi^2 F_5(x_t) + \frac{1}{32} (FF^\dagger)_{11}^2, \text{ for } j = k = 3. \end{cases}
\end{aligned} \tag{49}$$

For heavy quarks inside the loop, the factors  $C_{33}^{L,R}$  are in the agreement with [20].

Regarding the neutrino oscillation data, one needs the limit on the coupling constants that appear in Eq. (19). From the branching ratio above, in the assumption that there is no accidental cancelation among the various contributions, so that one can omit terms like  $Y_{13}^* Y_{23} Y_{jk}$  or  $F_{13} F_{23}^* F_{jk}$  with  $j, k = 1, 2$ , one gets, for a LQ mass of 1 TeV,

$$|Y_{13} Y_{23}| < 7.6 \times 10^{-3}, \quad |F_{13} F_{23}^*| < 1.8 \times 10^{-3} \tag{50}$$

if  $|F_{13}| \ll e$  and

$$|F_{13} F_{23}| < 1.3 \times 10^{-3} \tag{51}$$

if  $|F_{13}| \sim 1$ .

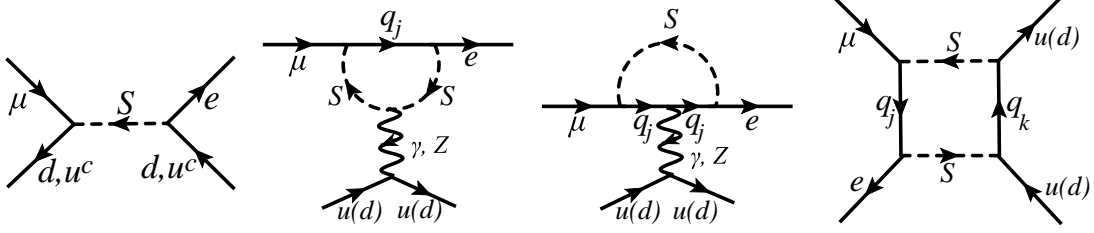


Figure 7: The diagrams leading to  $\mu - e$  conversion.  $q_j$  and  $S$  represent  $d_j$  ( $u_j^c$ ) quarks and  $\omega^{2/3}$  ( $\chi^{1/3}$ ) respectively.

### 3.3 $\mu - e$ Conversion in the nuclei

Another lepton flavor violating process that may occur in this model is  $\mu - e$  conversion in nuclei ( $\mu N \rightarrow eN$ ). The interesting type is the so-called coherent conversion in which the nucleus does not change its initial state [21]. In this section we shall discuss the implications of our model in such processes. It turns out that there exist tree level diagrams in addition to the one-loop diagrams (Fig. 7). These two sets of diagrams probe different Yukawa couplings. The loop diagrams involve the same couplings that appear in the neutrino mass matrix, and has to be given special attention. These loop diagrams are similar to  $\mu^- \rightarrow e^+e^-e^-$  except the pair of up/down quark is attached to the photon and  $Z$  lines. Following [18], the branching ratio of this process is given by

$$\text{BR}(\mu N \rightarrow eN) = \frac{|\vec{p}_e| E_e m_\mu^3 G_F^2 \alpha^3 Z_{\text{eff}}^4 F_p^2}{8\pi^2 Z \Gamma_N} |g_L^u(A + Z) + g_L^d(2A - Z) + 2Z\Delta g_L|^2 + L \leftrightarrow R, \quad (52)$$

where  $|\vec{p}_e|$  and  $E_e$  are the momentum and energy of the outgoing electron respectively,  $Z$  is the atomic number of the nucleus,  $A$  is the mass number of the nucleus,  $Z_{\text{eff}}$  is the effective atomic number defined in [22],  $F_p$  is the nuclear matrix element defined in [18, 21, 22],  $\Gamma_N$  is the muon capture rate of nucleus  $N$ , and  $g_{L,R}^{u,d}$  are defined as

$$\begin{aligned} g_L^u &= \eta_L \left( \frac{1}{4} - Q_u \sin^2 \theta_W \right), \quad g_R^d = \eta_R \left( \frac{1}{4} - Q_d \sin^2 \theta_W \right), \\ g_L^d &= \eta_L \left( \frac{1}{4} - Q_d \sin^2 \theta_W \right) + \frac{3\sqrt{2}Y_{11}^* Y_{21}}{4m_\omega^2 G_F} - \frac{3\sqrt{2}}{32\pi^2 G_F} \frac{(YY^\dagger)_{11}(YY^\dagger)_{21}}{4m_\omega^2}, \\ g_R^u &= \eta_R \left( \frac{1}{4} - Q_u \sin^2 \theta_W \right) + \frac{3\sqrt{2}F_{11} F_{21}^*}{4m_\chi^2 G_F} - \frac{3\sqrt{2}}{32\pi^2 G_F} \frac{(FF^\dagger)_{11}(FF^\dagger)_{12}}{4m_\chi^2}, \\ \Delta g_L &= \frac{2\sqrt{2}\alpha\pi}{G_F m_\mu^2} (f_{E0}(-m_\mu^2) + f_{M1}(-m_\mu^2) + f_{M0}(-m_\mu^2) + f_{E1}(-m_\mu^2)), \\ \Delta g_R &= \frac{2\sqrt{2}\alpha\pi}{G_F m_\mu^2} (f_{E0}(-m_\mu^2) + f_{M1}(-m_\mu^2) - f_{M0}(-m_\mu^2) - f_{E1}(-m_\mu^2)). \end{aligned} \quad (53)$$

Element	BR	$Z_{\text{eff}}$	$F_p$	Constraint
$^{48}\text{Ti}$	$< 4.3 \times 10^{-12}$	17.61	0.53	$\left  \frac{a_j^L Y_{ij}^* Y_{2j}}{m_\omega^2} + \frac{a_j^R F_{1j} F_{2j}^*}{m_\chi^2} \right ^2 + \left  \frac{b_j^L Y_{ij}^* Y_{2j}}{m_\omega^2} + \frac{b_j^R F_{1j} F_{2j}^*}{m_\chi^2} \right ^2 < \frac{5.2 \times 10^{-16}}{\text{GeV}^4}$
$^{208}\text{Pb}$	$< 4.6 \times 10^{-11}$	33.81	0.15	$\left  \frac{a_j^L Y_{ij}^* Y_{2j}}{m_\omega^2} + \frac{a_j^R F_{1j} F_{2j}^*}{m_\chi^2} \right ^2 + \left  \frac{b_j^L Y_{ij}^* Y_{2j}}{m_\omega^2} + \frac{b_j^R F_{1j} F_{2j}^*}{m_\chi^2} \right ^2 < \frac{9.7 \times 10^{-14}}{\text{GeV}^4}$

Table 2: The summary of  $\mu - e$  conversion for Ti and Pb. The values of  $Z_{\text{eff}}$  and  $F_p$  are taken from [21] whereas  $\Gamma_N$  are from [23].

Here  $Q_u$  and  $Q_d$  are the charges of the up- and down-quarks. As before, we can neglect terms proportional to  $\eta_L$  and  $F_3(x_{d_j})$ . The summary of constraints from this process is given in Table 2, with

$$\begin{aligned}
a_j^L &= (2A - Z) [32\pi^2 \delta_{1j} - (YY^\dagger)_{11}], \quad a_j^R = 2Ze^2 \tilde{h}_j, \quad b_j^L = 2Ze^2 \tilde{g}_j, \\
b_j^R &= (A + Z) [32\pi^2 \delta_{1j} - (FF^\dagger)_{11}] + 2Ze^2 F_4(x_{u_j}) \\
&\quad + 8\sqrt{2} G_F m_\chi^2 F_5(x_t) \left( \frac{3}{4}A - Z \sin^2 \theta_W \right) \delta_{3j},
\end{aligned} \tag{54}$$

where  $\tilde{g}_j = g_j|_{q^2=-m_\mu^2}$  and  $\tilde{h}_j = h_j|_{q^2=-m_\mu^2}$ . Here we take  $|\vec{p}_e| \simeq E_e \simeq m_\mu$ .

For  $^{48}\text{Ti}$ , we get for LQ mass of 1 TeV,  $|Y_{13}^* Y_{23}| < 4.6 \times 10^{-3}$  and  $|F_{13} F_{23}^*| < 1.9 \times 10^{-4}$  which are slightly stronger than the constraints from  $\mu^- \rightarrow e^+ e^- e^-$ . The tree-level diagrams alone give  $|Y_{11}^* Y_{21}| < 10^{-6}$  and  $|F_{11} F_{21}^*| < 10^{-6}$ . A new generation experiment called COMET has been proposed to reach a better sensitivity of  $10^{-16}$  [24]. There is also discussion of testing  $\mu - e$  conversion at a future Fermilab experiment. The prospects for these experiments observing new physics are good within our model. This is true even if the MEG experiment [25] obtains negative results for the  $\mu \rightarrow e\gamma$  decay.<sup>5</sup>

We can use the bound from  $\mu - e$  conversion and neutrino mass fitting to predict the minimum branching ratio for  $\mu \rightarrow 3e$ . Such a correlation is not possible for  $\mu \rightarrow e\gamma$  because of the GIM-like cancelation that occurs there, and the fact that  $F_{1j}$  is not constrained by neutrino data. Note that,  $Y_{i3}$  (assuming that only the bottom quark mediates the process) cannot be smaller than  $10^{-4}$  for LQ mass of 300 GeV, or else the induced neutrino mass will be too small. Therefore, the smallest branching ratio for  $\mu \rightarrow 3e$  can be predicted which is presented in Fig. 8. We see that  $\mu \rightarrow 3e$  can be substantial for a significant part of the parameter space.

<sup>5</sup>There is a class of model where  $\mu - e$  conversion is log-enhanced compared to  $\mu \rightarrow e\gamma$ , see Ref. [26].

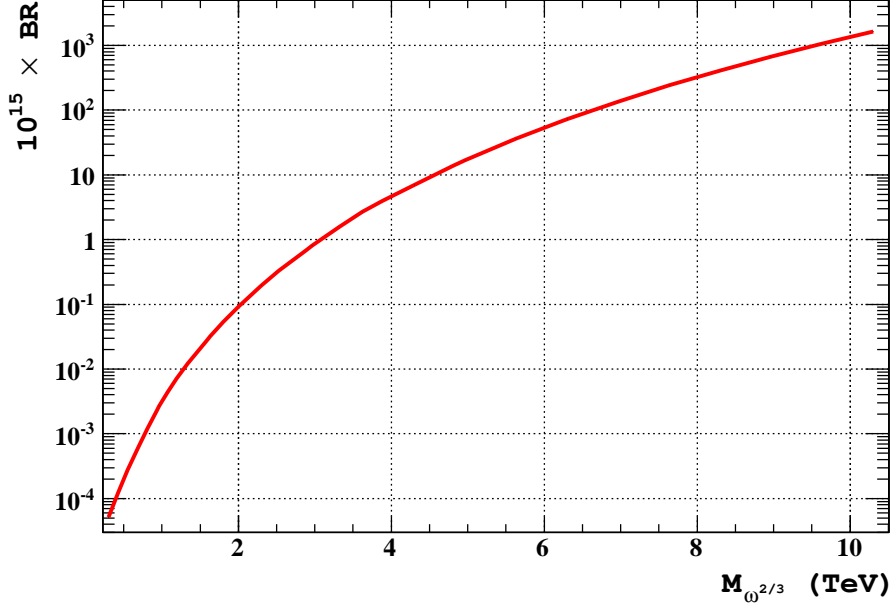


Figure 8: The smallest branching ratio for  $\mu \rightarrow 3e$  as suggested by neutrino mass fitting and  $\mu - e$  conversion.

### 3.4 $\tau^- \rightarrow e^- \eta$ and $\tau^- \rightarrow \mu^- \eta$ decays

It turns out that some of the potentially large entries in the neutrino mass matrix are eliminated from the constraints from the decays  $\tau^- \rightarrow e^- \eta$  and  $\tau^- \rightarrow \mu^- \eta$ . These processes can be mediated by  $\omega^{2/3}$  leptoquark at tree level. Here we ignore  $\eta - \eta'$  mixing and work in the  $SU(3)$  flavor symmetric limit. The branching ratios for these processes are given by

$$\begin{aligned} \text{BR}(\tau^- \rightarrow e^- \eta) &= \frac{1}{512\pi^2} \frac{|Y_{12}Y_{32}|^2 f_\eta^2 m_\tau^3}{m_\omega^4 \Gamma_{\text{total}}}, \\ \text{BR}(\tau^- \rightarrow \mu^- \eta) &= \frac{1}{512\pi^2} \frac{|Y_{22}Y_{32}|^2 f_\eta^2 m_\tau^3}{m_\omega^4 \Gamma_{\text{total}}}. \end{aligned} \quad (55)$$

We use  $f_\eta = 160$  MeV and data from [11] to derive

$$\begin{aligned} |Y_{12}Y_{32}| &< 1.2 \times 10^{-2} \left( \frac{m_\omega}{300 \text{ GeV}} \right)^2, \\ |Y_{22}Y_{32}| &< 1.0 \times 10^{-2} \left( \frac{m_\omega}{300 \text{ GeV}} \right)^2. \end{aligned} \quad (56)$$

### 3.5 Muon anomalous magnetic moment

The muon anomalous magnetic moment receives correction from the leptoquark exchange in our model and is given by

$$\delta(g-2)_\mu = 3.9 \times 10^{-10} \left( \frac{300 \text{ GeV}}{m_\chi} \right)^2 \left( \left| \frac{F_{21}}{1.0} \right|^2 + \left| \frac{F_{22}}{1.0} \right|^2 - F_4(x_t) \left| \frac{F_{23}}{1.0} \right|^2 \right). \quad (57)$$

Again, for the same reason as in the case of  $\mu \rightarrow e\gamma$ ,  $Y_{ij}$  couplings are practically have no effects here. By comparing the new contributions with the  $3\sigma$  anomaly in the experimental value,  $\delta(g-2)_\mu^{\text{exp}} = (24.6 \pm 8.0) \times 10^{-10}$  [27, 28], we see that this model can reduce or eliminate the discrepancy for order one values of the couplings  $F_{21}$  and  $F_{22}$ .

### 3.6 Upsilon Decay

Lepton number violating  $\Upsilon$  decay can set limit on the couplings  $Y$ . The decays we consider are  $\Upsilon \rightarrow \mu^+\mu^-$  and  $\Upsilon \rightarrow \mu^+\tau^-$ . The former is generated by the s-channel photon exchange and the latter is generated by the t-channel  $\omega^{2/3}$  exchange. In our model the ratio of these two branching ratios is given by

$$\frac{\text{BR}(\Upsilon \rightarrow \mu^+\tau^-)}{\text{BR}(\Upsilon \rightarrow \mu^+\mu^-)} = \frac{1}{32} \frac{|Y_{23}^* Y_{33}|^2}{16\pi^2 \alpha^2} \left( \frac{m_\Upsilon}{m_\omega} \right)^4, \quad (58)$$

where  $m_\Upsilon$  is the  $\Upsilon$  mass. The upper limit of this ratio is  $2.5 \times 10^{-4}$  [29]. Therefore, we get less constrained value

$$|Y_{23}^* Y_{33}| < 8.0 \left( \frac{m_\omega}{300 \text{ GeV}} \right)^2. \quad (59)$$

### 3.7 $D_s^- \rightarrow \ell^- \nu$ decay

Another interesting feature of the leptoquarks is that they can mediate a lepton number violating  $D_s$  decay:  $D_s^- \rightarrow \ell^- \nu$ . Currently there is a discrepancy at the  $2.5\sigma$  level between the experimental value and theoretical predictions based on lattice evaluation of the decay constant  $f_{D_s}$ . The LQ exchange can resolve the discrepancy. This issue has been studied in the framework of MSSM with broken  $R$ -parity [27] and with leptoquarks [30]. It turns out that in this model this process occurs at tree level mediated by  $X_a^{-1/3}$  leptoquarks in addition to the SM process. Since the SM diagram leads to antineutrino final states, while the  $X_a$  mediating processes result in neutrinos, there is no interference between the two. We get

$$\begin{aligned} \text{BR}(D_s \rightarrow \ell \nu) &= \frac{m_{D_s}}{8\pi} \tau_{D_s} f_{D_s}^2 G_F^2 |V_{cs}|^2 \left[ 1 + \frac{|Y_{i2}^* F_{22}|^2}{128 M_1^4 G_F^2 |V_{cs}|^2} \sin^2 2\theta \left( 1 - \frac{M_1^2}{M_2^2} \right)^2 \right] \\ &\times \left( 1 - \frac{m_\ell^2}{m_{D_s}^2} \right)^2 m_\ell^2, \end{aligned} \quad (60)$$

and by using the data from lattice calculation,  $f_{D_s} = (241 \pm 3) \text{ MeV}$  [31] and experimental result,  $f_{D_s}^{\text{exp}} = (277 \pm 9) \text{ MeV}$  [11], we can write

$$|Y_{i2}^* F_{22}| < 1.6 \left( \frac{M_1}{300 \text{ GeV}} \right)^2 \left( \frac{150 \text{ GeV}}{\mu} \right). \quad (61)$$

There is a similar contribution to the decay  $\pi^- \rightarrow \mu^- \nu_e$ . From this process we find

$$\text{BR}(\pi^- \rightarrow \mu^- \nu_e) = \frac{|Y_{11} F_{21}^*|^2}{128 M_1^4 G_F^2} \sin^2 2\theta \left( 1 - \frac{M_1^2}{M_2^2} \right)^2. \quad (62)$$

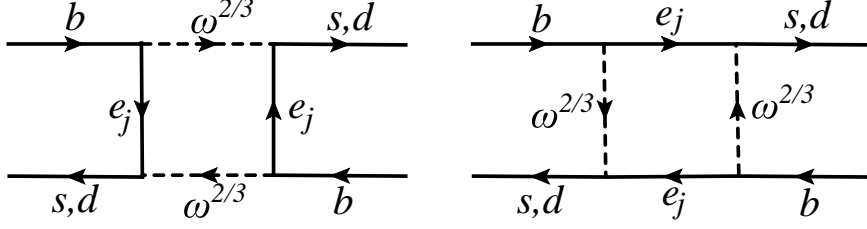


Figure 9: The box diagrams of  $B_s^- - \bar{B}_s$  Mixing.

By using experimental limits [11], one can derive

$$|Y_{11}F_{21}^*| < 1.0 \left( \frac{M_1}{300 \text{ GeV}} \right)^2 \left( \frac{150 \text{ GeV}}{\mu} \right). \quad (63)$$

### 3.8 New CP violation in $B_s - \bar{B}_s$ mixing

The leptoquarks of the model mediate meson–antimeson mixing via one-loop box diagrams. There is special interest in this process for the  $B_s$  system, as there are experimental hints for non-zero CP violation in this system. We find that the present model can nicely explain the new CP violation that would be needed in  $B_s - \bar{B}_s$  mixing, without generating unacceptable mixing in the  $B_d^0$ ,  $K^0$  and  $D^0$  systems.

The new effective Lagrangian for  $B_s - \bar{B}_s$  mixing in the models arising from the box diagrams of Fig. 9 is given by

$$\mathcal{L}_{\text{eff}}^{\text{new}} = -\frac{(Y_{i2}Y_{i3}^*)^2}{128\pi^2 m_\omega^2} (\bar{s}_R \gamma^\mu b_R) (\bar{s}_R \gamma_\mu b_R), \quad (64)$$

The hadronic matrix element for this operator is

$$\langle B_s | -\mathcal{L}_{\text{eff}}^{\text{new}} | \bar{B}_s \rangle = \frac{(Y_{i2}Y_{i3}^*)^2}{192\pi^2 m_\omega^2} m_{B_s} f_{B_s}^2 B_1^{B_s}(\mu) \eta_1^{B_s}(\mu), \quad (65)$$

where  $m_{B_s}$  and  $f_{B_s}$  are the  $B_s$  meson mass and decay constant respectively, whereas  $B_1^{B_s}(\mu)$  and  $\eta_1^{B_s}(\mu)$  are the bag parameter and QCD correction factor of Wilson coefficient defined in [32]. Both are evaluated at the scale  $m_b \sim 5 \text{ GeV}$ .

Similarly, one can have the same thing for other meson mixings

$$\begin{aligned} \langle B_d | -\mathcal{L}_{\text{eff}}^{\text{new}} | \bar{B}_d \rangle &= \frac{(Y_{i1}Y_{i3}^*)^2}{192\pi^2 m_\omega^2} m_{B_d} f_{B_d}^2 B_1^{B_d}(\mu) \eta_1^{B_d}(\mu), \\ \langle K | -\mathcal{L}_{\text{eff}}^{\text{new}} | \bar{K} \rangle &= \frac{(Y_{i2}Y_{i1}^*)^2}{192\pi^2 m_\omega^2} m_K f_K^2 B_1^K(\mu) \eta_1^K(\mu), \\ \langle D | -\mathcal{L}_{\text{eff}}^{\text{new}} | \bar{D} \rangle &= \frac{(F_{i1}F_{i2}^*)^2}{192\pi^2 m_\chi^2} m_D f_D^2 B_1^D(\mu) \eta_1^D(\mu). \end{aligned} \quad (66)$$

The Wilson coefficients correction can be found by following the procedures given in Ref. [32]. They are  $\eta_1^{s,d} = 0.80$ ,  $\eta_1^K = 0.76$ ,  $\eta_1^D = 0.78$ . Whereas the bag parameters are  $B_1^{s,d}(5 \text{ GeV}) = 0.86$ ,  $B_1^K(2 \text{ GeV}) = 0.66$ ,  $B_1^D(2.8 \text{ GeV}) = 0.865$ .

The limits on those couplings appearing in  $K - \bar{K}$ ,  $D - \bar{D}$ , and  $B_d - \bar{B}_d$  mixings can be derived by using  $m_K = 0.498 \text{ GeV}$ ,  $f_K = 0.16 \text{ GeV}$ ,  $m_D = 1.9 \text{ GeV}$ ,  $f_D = 0.2 \text{ GeV}$ ,  $m_{B_d} = 5.3 \text{ GeV}$  and  $f_{B_d} = 0.24 \text{ GeV}$ . They are

$$\begin{aligned} |Y_{i2}Y_{i1}| &< 6.3 \times 10^{-3} \left( \frac{m_\omega}{300 \text{ GeV}} \right), \\ |F_{i1}F_{i2}| &< 5.0 \times 10^{-3} \left( \frac{m_\chi}{300 \text{ GeV}} \right), \\ |Y_{i2}Y_{i3}| &< 1.1 \times 10^{-2} \left( \frac{m_\omega}{300 \text{ GeV}} \right). \end{aligned} \quad (67)$$

The combination of SM and this new contribution to  $B_s - \bar{B}_s$  system can be parameterized as [33]

$$M_{12} = M_{12}^{\text{SM}}(1 + h_s e^{2i\sigma_s}), \quad (68)$$

where  $h_s$  is the matrix element given in Eq. (65). When  $Y_{32} \sim 1$  and  $|Y_{33}/Y_{23}| \sim 2$  for  $M_1 = 300 \text{ GeV}$ , whereas  $\mu - e$  conversion suggests  $Y_{33} \simeq 0.024$  for  $m_\omega = 300 \text{ GeV}$ , the new contribution induced by this model can be as large as 94% correction to the SM one. Since there is CP violation in the mixing, our model can explain the experimental observations. The prediction for forthcoming experiments is the existence of leptoquarks with mass less than about 500 GeV. The central values of observations can be naturally obtained in our model.

### 3.9 Neutrinoless double beta decay

The light neutrino exchange contribution to neutrinoless double beta decay vanishes in our model, owing to the zero of the (1,1) entry in  $M_\nu$ . However, it can proceed via the vector-scalar exchange process, which does not need a helicity flip of the neutrino [34]. The relevant diagram is shown in Fig. (10). The effective Lagrangian of that process after Fierz rearrangement is

$$\mathcal{L}_{\text{eff}} = \frac{G_F^2}{2} \epsilon \bar{u}\gamma^\mu(1-\gamma_5)d \left[ \bar{u}(1+\gamma_5)d\bar{e}\gamma_\mu(1-\gamma_5)\frac{1}{\not{q}}e^c + \frac{1}{4}\bar{u}\sigma^{\alpha\beta}(1+\gamma_5)d\bar{e}\gamma_\mu(1-\gamma_5)\frac{1}{\not{q}}\sigma_{\alpha\beta}e^c \right], \quad (69)$$

where  $q$  is the internal neutrino momentum. The first term is the scalar-pseudoscalar current and the second one is the tensor current, and the parameter  $\epsilon$  is defined as

$$\epsilon = \frac{Y_{11}^* F_{11}}{2\sqrt{2}M_1^2 G_F} \sin 2\theta \left( 1 - \frac{M_1^2}{M_2^2} \right), \quad (70)$$

where  $\theta$  is the leptoquarks mixing angle. Following Päs *et al.* [35], the constraint on  $|Y_{11}^* F_{11}|$  is calculated by constructing nuclear matrix element in pn-QRPA model [36] and applying the



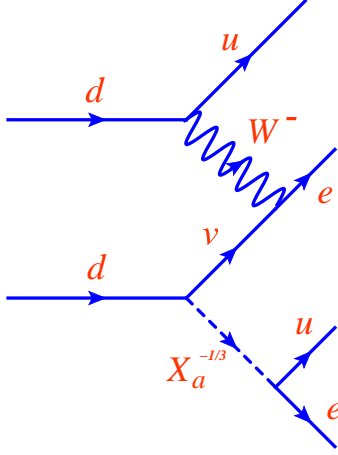


Figure 10: The neutrinoless double beta decay diagram generated by this model.

result of  $0\nu\beta\beta$  half life,  $T_{1/2}(0\nu\beta\beta) > 1.2 \times 10^{25}$  yr, obtained from Heidelberg-Moscow experiment [37]. A straightforward calculation gives

$$|Y_{11}^* F_{11}| < 1.7 \times 10^{-6} \left( \frac{M_1}{1 \text{ TeV}} \right)^2 \left( \frac{0.5 \text{ TeV}}{\mu} \right). \quad (71)$$

Here, both the scalar-pseudoscalar and tensor currents are taken into account. One sees that it is possible to observe neutrinoless double beta decay in the near future, even with hierarchical neutrino masses.

## 4 Collider signals

At hadron colliders, leptoquarks can be produced in pairs via quark-quark or gluon-gluon fusion and/or in association with lepton via quark-gluon fusion. The former depends on the QCD coupling constant and the latter depends on the  $|F_{i1}|^2$  and  $|Y_{i1}|^2$ . The associated production may be important if the  $F$  and  $Y$  are as large as electromagnetic coupling  $e$  [38]. Since these couplings are constrained by rare processes such as neutrinoless double beta decay, it seems unlikely that single production will be dominant in our model. Therefore, here we focus on pair production of leptoquarks.

In  $\omega^{2/3}$  pair production, each will decay to a charged lepton and a down quark with opposite charges. The resulting final state is two leptons and two jets. At the LHC with  $\sqrt{s} = 14$  TeV and mass of leptoquark equals to 500 GeV, the cross section is about 340 fb [38], decreasing to 4.2 fb for a LQ mass of 1 TeV. The dominant background for this process is final states from  $Z + \text{jets}$  and  $\bar{t}t$  production. For high leptoquark mass, only  $Z + \text{jets}$  is dominant. LHC can probe this leptoquark mass up to 1.2 TeV with integrated luminosity of  $300 \text{ fb}^{-1}$ .

In  $X_a^{-1/3}$  pair production, there are two possible signals. First, each  $X_a^{-1/3}$  decays to up-quark and a lepton, leading to two lepton and two jets signal. Secondly, one  $X_a^{-1/3}$  decays to charged

lepton and up quark and the other one decays to neutrino and a down-type quark, leading to one lepton plus jets plus missing energy. The first signature is similar to the  $\omega^{2/3}$  case. The second one has dominant background coming from  $W + \text{jets}$  and  $\bar{t}t$  production. In Ref. [38], it has been shown that LHC can probe this leptoquark mass up to 1.2 TeV with integrated luminosity of  $300 \text{ fb}^{-1}$ .

The decays of the  $\omega^{2/3}$  leptoquark into  $e^+b$ ,  $\mu^+b$ ,  $\tau^+b$  will occur in the following ratios:

$$\Gamma(\omega^{2/3} \rightarrow e^+b) : \Gamma(\omega^{2/3} \rightarrow \mu^+b) : \Gamma(\omega^{2/3} \rightarrow \tau^+b) = |y|^2 : |z|^2 : 1 . \quad (72)$$

Measurement of any one of these branching ratios will determine the CP violating phase  $\delta$  via Eq. (25). This can of course be cross checked in long baseline neutrino oscillation experiments, especially since  $\sin^2 \theta_{13}$  is large. If two branching ratios in the decay of  $\omega^{2/3}$  are measured, that will determine the phase  $\delta$  in two different ways, allowing for another consistency check.

The leptoquarks  $X_a^{-1/3}$ , ( $a = 1, 2$ ) which are linear combinations of  $\chi^{-1/3}$  and  $\omega^{-1/3}$  will decay into charged leptons in the following ratios:

$$\Gamma(X_a^{-1/3} \rightarrow \mu^-t) : \Gamma(X_a^{-1/3} \rightarrow \tau^-t) = |x|^2 : 1 . \quad (73)$$

Note that this result holds for both  $X_a^{-1/3}$ , independent of the  $(\omega^{-1/3} - \chi^{-1/3})$  mixing angle  $\theta$ . Measuring this branching ratio will determine  $|x|$ , providing another check for the model. Since numerically  $|x| \gg 1$ , we expect that at least one of the the  $X_a^{-1/3}$  will have  $\mu^-$  in the final state dominantly. It should be noted that the decay  $X_a^{-1/3} \rightarrow e^-t$  will be suppressed, owing to constraints from  $\mu \rightarrow e\gamma$ . Of course, these  $X_a^{-1/3}$  fields also decay into  $\bar{\nu}_i d_j$ . The lepton flavor composition in this mode would be near to impossible to determine.

## 5 Conclusion

In this paper we have presented a new two-loop neutrino mass generation model. This involves TeV scale leptoquarks, which can be directly tested at the LHC. The structure of the model is such that the neutrino mixing angle  $\sin^2 \theta_{13}$  is predicted to be close to the current experimental limit of 0.05. The neutrino oscillation parameters are closely linked to the decay properties of the leptoquarks. By measuring the branching ratios of the LQ bosons, in this model, one is measuring CP violating phase  $\delta$  of neutrino oscillations. These measurements also provide a number of cross checks by which the model can be falsified.

We have discussed various rare decay processes mediated by the LQ bosons. The process  $\mu^- \rightarrow e^- \gamma$  may very well be suppressed, owing to a GIM-like mechanism, while the decay  $\mu^- \rightarrow e^+ e^- e^-$  and  $\mu - e$  conversion in nuclei are within reach of the next generation experiments. A very interesting feature of the model is that the present hint of new physics contributions to CP violation in  $B_s - \bar{B}_s$  mixing fits rather well here, without conflicting other well-measured

meson mixings. Neutrinoless double beta decay can occur via LQ exchange, even when the neutrino spectrum has a normal hierarchy. Near future experiments will have a lot to say on the consistency of the model.

## Acknowledgment

This work is supported in part by US Department of Energy Grant Numbers DE-FG02-04ER41306 and DE-FG02-ER46140.

## References

- [1] P. Minkowski, Phys. Lett. **B67**, 421 (1977); M. Gell-Mann, P. Ramond, and R. Slansky, in *Supergravity*, eds. D. Freedman *et al.*, (North-Holland, Amsterdam, 1980); T. Yanagida, in *Proceedings of the Workshop on Baryon Number in the Universe*, eds. O. Sawada and A. Sugamoto, (KEK, 1979); R. Mohapatra and G. Senjanović, Phys. Rev. Lett. **44**, 912 (1980).
- [2] A. Zee, Phys. Lett. **B93**, 389 (1980).
- [3] For phenomenological analyses see: A. Y. Smirnov and M. Tanimoto, Phys. Rev. D **55**, 1665 (1997).
- [4] X. G. He, Eur. Phys. J. C **34**, 371 (2004).
- [5] A. Zee, Nucl. Phys. B **264**, 99 (1986).
- [6] K. S. Babu, Phys. Lett. **B203**, 132 (1988).
- [7] K. S. Babu and C. Macesanu, Phys. Rev. D **67**, 073010 (2003); M. Nebot, J. F. Oliver, D. Palao and A. Santamaria, Phys. Rev. D **77**, 093013 (2008).
- [8] K. S. Babu and C. N. Leung, Nucl. Phys. **B619**, 667 (2001).
- [9] D. Aristizabal Sierra, M. Hirsch and S. G. Kovalenko, Phys. Rev. D **77**, 055011 (2008).
- [10] W. Buchmuller and D. Wyler, Phys. Lett. B **177**, 377 (1986); W. Buchmuller, R. Ruckl and D. Wyler, Phys. Lett. B **191**, 442 (1987) [Erratum-ibid. B **448**, 320 (1999)].
- [11] Particle Data Group, C. Amsler *et al.*, Phys. Lett. **B667**, 1 (2008).
- [12] K. S. Babu, Y. Meng and Z. Tavartkiladze, arXiv:0812.4419 [hep-ph] and references therein.
- [13] T. Schwetz, M. A. Tortola, and J. W. F. Valle, New J. Phys. **10**, 113011 (2008).

- [14] V. M. Abazov *et al.* [D0 Collaboration], arXiv:1005.2222 [hep-ex]. D. E. Acosta *et al.* [CDF Collaboration], Phys. Rev. D **72**, 051107 (2005); V. M. Abazov *et al.* [D0 Collaboration], Phys. Rev. D **71**, 071104 (2005); A. Abulencia *et al.* [CDF Collaboration], Phys. Rev. D **73**, 051102 (2006); V. M. Abazov *et al.* [D0 Collaboration], Phys. Lett. B **636**, 183 (2006).
- [15] A. Dighe, A. Kundu and S. Nandi, arXiv:1005.4051 [hep-ph].
- [16] P. H. Frampton, S. L. Glashow and D. Marfatia, Phys. Lett. B **536**, 79 (2002).
- [17] Z. z. Xing, Phys. Lett. B **530**, 159 (2002).
- [18] Y. Kuno and Y. Okada, Rev. Mod. Phys. **73**, 151 (2001).
- [19] L. Lavoura, Eur. Phys. J. C **29**, 191 (2003).
- [20] J. Hisano, T. Moroi, K. Tobe, and M. Yamaguchi, Phys. Rev. D **53**, 2442 (1996); E. Arganda and M. J. Herrero, Phys. Rev. D **73**, 055003 (2006); J. Hisano and D. Nomura, Phys. Rev. D **59**, 116005 (1999).
- [21] A. Czarnecki, W. J. Marciano, and K. Melnikov, AIP Conf. Proc. **435**, 409 (1998).
- [22] H. C. Chiang, E. Oset, T. S. Kosmas, A. Faessler, and J. D. Vergados, Nucl. Phys. A **559**, 526 (1993).
- [23] M. Eckhause, R. J. Harris, and W. B. Shuler, Phys. Lett. **19**, 348 (1965).
- [24] Y. G. Cui *et al.* [COMET Collaboration], KEK-2009-10, Jun 2009.
- [25] M. Grassi [MEG Collaboration], Nuovo Cim. **032C**, 223 (2009).
- [26] M. Raidal and A. Santamaria, Phys. Lett. B **421**, 250 (1998).
- [27] G. Bhattacharyya, K. B. Chatterjee, and S. Nandi, Nucl. Phys. B **831**, 344 (2010).
- [28] J. Prades, Acta Phys. Polon. Supp. **3**, 75 (2010).
- [29] W. Love *et al.*, Phys. Rev. Lett. **101**, 201601 (2008).
- [30] B. A. Dobrescu and A. S. Kronfeld, Phys. Rev. Lett. **100**, 241802 (2008); R. Benbrik and C. H. Chen, Phys. Lett. B **672**, 172 (2009); I. Dorsner, S. Fajfer, J. F. Kamenik, and N. Kosnik, Phys. Lett. B **682**, 67 (2009).
- [31] E. Follana, C. T. H. Davies, G. P. Lepage and J. Shigemitsu [HPQCD Collaboration and UKQCD Collaboration], Phys. Rev. Lett. **100**, 062002 (2008); T. Onogi, Int. J. Mod. Phys. A **24**, 4607 (2009).

- [32] D. Becirevic, V. Gimenez, G. Martinelli, M. Papinutto and J. Reyes, JHEP **0204**, 025 (2002); M. Ciuchini *et al.*, JHEP **9810**, 008 (1998); M. Bona *et al.* [UTfit Collaboration], JHEP **0803**, 049 (2008); K. S. Babu and Y. Meng, Phys. Rev. D **80**, 075003 (2009).
- [33] Z. Ligeti, M. Papucci, G. Perez and J. Zupan, arXiv:1006.0432 [hep-ph].
- [34] K. S. Babu and R. N. Mohapatra, Phys. Rev. Lett. **75**, 2276 (1995).
- [35] H. Päs, M. Hirsch, and H. V. Klapdor-Kleingrothaus, Phys. Lett. **B459**, 450 (1999).
- [36] K. Muto, E. Bender, and H. V. Klapdor, Z. Phys. **A334**, 177,187 (1989); M. Hirsch, K. Muto, T. Oda, and H. V. Klapdor-Kleingrothaus, Z. Phys. **A347**, 151 (1994).
- [37] L. Baudis *et al.*, Phys. Lett. B **407**, 219 (1997).
- [38] A. Belyaev, C. Leroy, R. Mehdiyev and A. Pukhov, JHEP, **0509**, 005 (2005).